

# Molecular Subtypes Based on DNA Methylation Predict Prognosis in Lung Squamous Cell Carcinoma

XiuShen Li

Guangzhou University of Chinese Medicine <https://orcid.org/0000-0002-7135-7299>

Ke-Chao Nie

Guangzhou University of Chinese Medicine

Zhi-Hua Zheng

Guangzhou University of Chinese Medicine

Rui-Sheng Zhou

Guangzhou University of Chinese Medicine

Yu-Sheng Huang

Guangzhou University of Chinese Medicine

Zeng-Jie Ye

Guangzhou University of Chinese Medicine

Fan He

Guangzhou University of Chinese Medicine

Ying Tang (✉ [18825144748@163.com](mailto:18825144748@163.com))

<https://orcid.org/0000-0001-5666-8139>

---

## Research article

**Keywords:** Lung squamous cell carcinoma, DNA methylation, molecular subtype, TCGA, prognosis

**Posted Date:** October 15th, 2020

**DOI:** <https://doi.org/10.21203/rs.3.rs-80105/v1>

**License:**   This work is licensed under a Creative Commons Attribution 4.0 International License.

[Read Full License](#)

---

**Version of Record:** A version of this preprint was published on January 23rd, 2021. See the published version at <https://doi.org/10.1186/s12885-021-07807-7>.

# Abstract

**Background:** Due to tumor heterogeneity, the diagnosis, treatment, and prognosis of patients with lung squamous cell carcinoma (LUSC) are difficult. DNA methylation can affect tumor heterogeneity by participating in gene expression.

**Methods:** In this study, we collected the clinical information of LUSC patients in the Cancer Genome Atlas (TCGA) database and the relevant methylated sequences of the University of California Santa Cruz (UCSC) database to construct methylated subtypes and performed prognostic analysis.

**Results:** 965 potential independent prognosis methylation sites were finally identified and the genes were identified. Based on consensus clustering analysis, seven subtypes were identified by using 965 CpG sites and corresponding survival curves were plotted. The prognostic analysis model was constructed according to the methylation sites' information of the subtype with the best prognosis. Internal and external verifications were used to evaluate the prediction model.

**Conclusions:** Models based on differences in DNA methylation levels may help to classify the molecular subtypes of LUSC patients, and provide more individualized treatment recommendations and prognostic assessments for different clinical subtypes. GNAS, FZD2, FZD10 are the core three genes that may be related to the prognosis of LUSC patients.

## 1. Background

Lung cancer, the most commonly diagnosed cancer (11.6%), is the leading cause of cancer death, which accounts for 18.4% of cancer deaths among men and women[1]. The incidence of lung cancer is increasing rapidly, causing a huge economic burden. Approximately 66 % patients have lost the opportunity to undergo radical surgery after the diagnosis of lung cancer in China[2]. Non-small cell lung cancer (NSCLC), a heterogeneous disease, accounts for more than four-fifths of all lung cancers, and the pathological classification and clinical stage of patients are closely related to their prognosis [3]. Patients with lung squamous cell carcinoma account for more than 30% of patients with non-small cell lung cancer[4].

In the past two decades, the epigenetic understanding of lung cancer has developed exponentially [5]. Epigenetic research has provided key data for the occurrence of lung cancer. DNA methylation is the presence of methyl groups at the CpG dinucleotides, which usually locates near the gene promoter and affects gene expressions[6]. Transcriptional silencing caused by hypermethylation of CpG islands has become a key factor in the occurrence and development of lung cancer[7]. Abnormal DNA methylation silences the expression of tumor suppressor genes (TSG) by methylation of the promoter regions [8, 9]. DNA methylation markers have important value in the early diagnosis of lung cancer, predicting the treatment effect and tracking the resistance of treatment. The methylation of p16INK4a and MGMT, which can be detected in the sputum of most LUSC patients, could be used to predict the risk of lung cancer in smokers [5]. However, a large number of lung squamous cell carcinoma patients have not been

screened for abnormal methylation genes in the promoter region, and further analysis of their association with tumor classification and patient survival time.

In this research, based on the TCGA and UCSC databases, we screened out multiple DNA methylation biomarkers to construct and verify the prognostic prediction model, which could be used to provide more individualized treatment recommendations and prognostic assessments for different clinical subtypes.

## 2. Methods

### 2.1 Data download and preprocessing

Downloaded RNA sequencing data which came from 504 primary lung squamous cell neoplasms samples from the TCGA databases(<https://cancergenome.nih.gov/> 2020-07-08). Appendix S1 shows the clinical information of these 504 patient samples, including follow-up data. Downloaded the DNA methylation data of Illumina Infinium HumanMethylation450 and 27 BeadChip arrays, which were applied on samples of 503 and 150 patients from UCSC Cancer Database(2020-07-09), respectively.

This study only includes sample data with clinical follow-up times exceeding 30 days.  $\beta$ -value ranging from 0 (unmethylated) to 1 (fully methylated) represented the DNA methylation level of each site. Use the “impute” and “sva” packages in R language to eliminate the effect of batch effect. CpG sites were filtered by using the next 4 processes:(1) Remove the CpG sites with data less than 30% of samples.(2) Remove the unstable CpG sites which located on single nucleotide polymorphisms and sex chromosomes.(3)Since DNA methylation in the promoter region extremely affects gene expression, only the CpG sites in the promoter region (2 kb upstream to 0.5 kb downstream from the transcription start site) were retained.(4) Remove the CpG sites which in the Illumina Infinium HumanMethylation 450 microarray existed the polymorphic CpG and cross-reactive probes.(5)CpG sites which existed in the DNA methylation data of the downloaded Illumina Infinium HumanMethylation 27 and 450 BeadChip arrays were retained. Finally, 477 samples and 21123 methylation sites were selected for further analysis.

The data from HumanMethylation 450 microarray is classified as the training cohort, and the data from 27 BeadChip is classified as the external test cohort. Appendix S2 and 3 show the methylation site profiles and clinical information (age, survival time, gender, grade, and TNM stage) of the two cohorts, respectively.

### 2.2 Selecting characteristic CpG sites through COX proportional risk regression models

LUSC molecular subtypes may affect the prognosis of patient samples, so CpG sites, which effected survival significantly were used to distinguish subtypes. CpG sites were selected by using the next 3 processes:(1) For each CpG site, TNM stage, age, gender and survival data, use methylation levels to construct a univariate Cox proportional risk regression model. (2) Introduce Sites with significantly different levels of methylation expression( $p \leq 0.05$ ) from univariate Cox proportional hazards regression model into multivariate Cox proportional risk regression models constructed from TNM staging, age,

gender and survival data.(3) Select the characteristic CpG sites which are significant in multivariate and univariate Cox regression analysis.

### **2.3 Identification molecular subtypes related to prognosis**

Based on the CpG sites with significantly different levels of methylation expression "ConsensusClusterPlus" package in R was used for consensus clustering to identify LUSC molecular subtypes. This algorithm expands consensus clustering algorithm is often used to create consensus values and evaluate the stability of identified clusters. This algorithm, one of the unsupervised class discovery algorithms, defined "consensus" clustering by estimating the stability of clustering results by applying a specific clustering means to the random subsets of data. In each iteration, sample 80% of the tumors data , and then utilize k-means algorithm which contained Euclidean square distance metric. After 100 iterations, we gained the project-consensus results and cluster consensus.

The heatmap of the consensus matrix which came from the graphical output results included the consensus cumulative distribution function (CDF) plots, delta area plots and clustering results. We can use the graphical results to determine the approximate number of clusters. According to the following criteria the sorts of clusters were determined: (1) The consistency within the cluster was high. (2) The coefficient of variation is relatively low. (3) The area under the CDF curve did not increase significantly. According to the following formula Calculate the coefficient of variation:  $CV = (SD / MN) * 100 \%$ , where SD and MN represented the standard deviation and the average number of samples, respectively. The area under the CDF curve was used to define the category number. Tend to use more categories for LUSC to get more detailed classification categories. Utilize the "pheatmap" R package to get heatmap which correspond to consensus clustering. Use a color gradient to indicate the consensus value from 0 (white) to 1 (dark blue); sort out the matrix so that the items which belongs to the same cluster can be put together. In this arrangement, the perfect consensus matrix will show a heatmap, which is displayed by the diagonal blue blocks on a white background.

### **2.4 Analyses of Survival and clinical characteristics**

Use Kaplan–Meier plots to demonstrate overall survival among LUSC subtypes which was determined by DNA methylation profiles. Utilize the log-rank test to assess the significance of differences among the subtypes. Use the "survival" R package to execute survival analyses. The chi-squared test was used to analysis the connection between DNA methylation clustering and both biological and clinical characteristics. All tests used two-sided, and only  $p < 0.05$  was thought statistically significant.

### **2.5 GO and KEGG enrichment analysis**

The "clusterProfiler" and "ggplot2" R package combined with Gene Ontology (GO) and Kyoto Encyclopedia of Genes and Genomes (KEGG) database were applied to process gene enrichment analysis of the biological process, cell component, molecular function and biological pathways.

### **2.6 Construction and testing of the prognostic prediction model**

Based on the prognostic information of patients and methylation profiles of 26 CpG sites, Use the "survival" R package to construct and verify the Cox proportional hazards model. The formula of the model is:  $\text{risk score} = \text{cg01775414} * 7.35 - \text{cg03522063} * 1.71 - \text{cg03954587} * 0.65 + \text{cg05158615} * 0.49 - \text{cg06918467} * 0.55 - \text{cg07850604} * 0.08 - \text{cg09339527} * 0.46 - \text{cg10332700} * 0.07 - \text{cg11814446} * 1.64 + \text{cg11846236} * 2.60 + \text{cg13739417} * 2.52 - \text{cg14776962} * 0.38 - \text{cg15001381} * 6.07 - \text{cg17619823} * 0.12 + \text{cg19255783} * 0.10 + \text{cg20855565} * 0.05 - \text{cg21331821} * 0.33 + \text{cg21663122} * 1.51 - \text{cg23054883} * 3.52 + \text{cg24402880} * 0.42 + \text{cg24892510} * 0.90 - \text{cg25228126} * 0.08 + \text{cg25533774} * 0.56 - \text{cg25856383} * 0.93 - \text{cg25983380} * 0.30 - \text{cg27654142} * 1.88$ . Internal verification randomly divided the data from the 450k BeadChip into an internal training cohort and an internal testing cohort for verification, while external verification used all data of the 450k BeadChip as the external training cohort and all data of the 27k BeadChip as the external testing cohort.

The cBio Cancer Genomics Portal (<http://www.cbioportal.org/2020-07-10>) is an open platform that provides information for analyzing and visualizing large-scale cancer genomics. We probed the genetic alterations connected with the 24 genes corresponding to 26 prognostic-related methylation sites, and the correlation between mRNA and DNA methylation by utilizing the cBioPortal tool. The clinical characteristics and prognosis model of the patient were used as different influencing factors, and the prognostic information of the patient was analyzed by univariate and multivariate cox analyses , and the corresponding ROC curve is drawn.

## 3. Results

### 3.1 Select potential methylation sites associated with the prognosis of patients

After preprocess the downloaded patients data according to the description in Materials and Methods, we identified 21,122 methylation sites. Then, the patients were divided into two cohorts, namely the training cohort and the test cohort, and detailed patient data is shown in the Appendix S2-3. With  $p < 0.05$  as the screening condition, the univariate Cox regression analysis was used to select the CpG sites, which could be used to serve as potential DNA methylation biomarkers for overall survival of patients with LUSC. Finally, obtain 1160 related CpG sites(Appendix S4).The T, N, M, stage and age as covariates Multivariate Cox regression analysis was performed on 1160 methylation sites, and 965 independent CpG sites, which were considered potential prognostic methylation sites were identified(Appendix S5).

### 3.2 Consensus clustering to identify different subtypes of DNA methylation prognosis and prognostic analysis among subtypes

The consensus clustering of 965 potential prognostic methylation sites were utilize to identify different subtypes of LUSC for prognostic purposes. The amounts of clusters were decided by using the next 2 standards: (1) The consistency within the cluster is high. (2) The area under the CDF curve is not increase significantly. Based on the category number, the average clustering consensus was calculated. As shown in Figures 1A and B, after six categories the area under the curve of CDF started to stabilize. We chose a larger number of clusters to increase the prognostic value of LUSC subtypes. Next, we also utilized the

consensus matrix to decide the optimal amount of subtypes. As shown in Figure 2A, the consensus matrix, which showed a well-defined block structure represented the consensus of 7. DNA methylation subtypes, stage, age and TNM category are displayed as annotations in Figure 2B which corresponds to the dendrogram of the Figure 2A.

The Kaplan-Meier survival analysis showed significant differences in prognosis between the 7 subtypes ( $p < 0.001$ ). The proportions were shown in Figure 3A–3F. The correlation tendencies among the 7 clusters were shown in the figure: (1) Cluster 4 had the smallest proportion of patients over 65 years of age, while Cluster 7 had the highest proportion of patients over 65 years of age. (2) The proportion of female patients in cluster 2 was the largest, while the proportion of female patients in cluster 6 is the smallest. (3) Cluster 7 has the largest proportion of patients in stage I, and Cluster 5 had the smallest proportion of patients in stage I. (4) Cluster 4 had the largest proportion of patients with T1. (5) Cluster 7 had the largest proportion of patients with N0, and Cluster 5 had the smallest proportion of patients with N0. (6) Almost all patients did not have distant metastasis. These tendencies revealed that each clinical parameter had a different ratio among 7 clusters. As shown in Figure 3G, cluster 5 has the worst prognosis, while cluster 7 has the best prognosis. Then based on the clinical information of age, gender, stage score, topography score, lymphocyte infiltration and metastasis, we analyzed intra-subtype ratio for the 7 subtypes.

### **3.3 Recognize different features according to DNA methylation clustering and selecting the cluster-specific methylation sites**

Though the above-mentioned genome annotations for the 965 CpG sites, we identified 1037 corresponding promoter genes altogether. Next these 1037 genes were identified 27 significant enrichment pathways ( $P < 0.05$ ) which were displayed in Figure 4 and Appendix S6 by processing KEGG pathway enrichment analysis. Cell cycle, Fc gamma R-mediated phagocytosis, Non-homologous end-joining, Protein digestion and absorption, Cellular senescence was the top five pathways with significant differences. Using "enrichplot" R package to analysis the crosstalk of pathways identified by KEGG pathway enrichment analysis (Figure 4B). Renal cell carcinoma, chronic myelogenous leukemia, and FoxO signaling pathway were the three most connected pathways with other signaling pathways.

Then, we selected the cluster-special methylation sites by including the CPG methylation sites as features of the clusters. 965 genes in 266 external training data set samples were available. The gene expression heat map is shown in Figure 4C, and the original data is shown in Appendix S7. As description of Materials and Methods, analyze the differences between the 7 clusters at each methylation sites (Appendix S8). 41 cluster-special methylation sites identified was displayed in Appendix S9. Enrichment analysis of KEGG signaling pathway was performed to analysis genes corresponding to 41 cluster-special methylation sites (Figure 5B). The enrichment analysis of KEGG signaling pathways resulted in 30 related signaling pathways. Analysis of the genes that make up the pathway revealed that the genes GNAS, FZD2, FZD10, GNG4, and AXIN1 participated in the most relevant pathways. Genome annotations of the 41 specific sites were used to identify their corresponding genes (Appendix S10). The analysis of the 10 signaling pathways with the smallest p-values revealed that these 46 genes were related to

diseases such as Basal cell carcinoma, Breast cancer, Gastric cancer, etc., and pathway such as Signaling pathways regulating pluripotency of stem cells, Hippo signaling pathway, Wnt signaling pathway.

The 30 signal pathways obtained by enrichment analysis were only enriched in Clusters 1, 2, 4, and 6 (Appendix S11). Cluster 7 has the lowest methylation level among all clusters, while cluster 5 has the highest methylation level (Figure 1C).

### 3.4 Construction and evaluation of LUSC prognostic model

Cluster 6 with 26 specific methylation sites was selected as the seedcluster, because it has a good prognosis and the largest number of specific methylation sites among clusters. For all samples in the Training cohort, the methylation levels of these 26 specific sites were obtained. Next, we built a multiCox risk regression model, and used this model to calculate the risk value of each patient. Utilizing the "survival" and "survminer" R package to plot survival curves, the results showed that there were significant differences between the two cohorts (Figure 6). Specifically, the prognosis of the high-risk cohort was poor, indicating that these specific methylation sites might be a sign of prognosis. The ROC analysis was performed using the risk score computed for each training cohort sample, and the results are shown in Figure 6A. The area under the curve (AUC) was 0.714, indicated that the model worked well. Then sort the samples by risk score and find that as the score increases, the risk of death is higher (Figure 6B). According to the cut-off risk score of -0.70491, the patients in the training cohort were divided into high-risk cohort and low-risk cohort evenly, and the heat map was used to show the methylation level of 26 special sites in the training cohort (Figure 6D).

Then, we used the caret R package to divide the patients in the external training cohort into two cohorts, namely the internal training cohort and the internal test cohort. We calculated the patient's risk value, and used the R language to draw the survival curve and ROC curve of the two cohorts of patients. As shown in Figure 7, the prognosis of patients in the high and low risk cohorts is statistically significant, and the p value was less than 0.001. The area under the curve (AUC) is 0.735 and 0.662, respectively, which is consistent with the results of the external training cohort.

Finally, the data of the patients in the testing cohort were collated to obtain the methylation levels of the patients at 26 special sites (Figure 8D), and the obtained prognostic model was applied to the patients in the external test cohort which came from the 27 BeadChip to calculate their risk scores. Using -0.70491 as the critical value, it was divided into high-risk cohort and low-risk cohort (Figure 8B). The prognosis of the low-risk cohort was significantly better than that of the advanced cohort (Figure 8C), and there was a significant difference between the two cohorts ( $p=0.03743$ ). Consistent with the results of the training cohort, it was proved that this model could be used to predict the prognosis of patients.

The alteration information of the 24 genes was showed in Figure 9. We found that the 24 genes were altered in 219 (43%) of the 511 sequenced cases/patients (511 total). The ADRB3 was altered most often (18%), including deep deletion, amplification, mRNA high, etc. The correlation between messenger RNA (mRNA) and DNA methylation of the 5 genes with highest degree of genetic alterations in the TCGA LUSC

patients was demonstrated in Figure 9C. We found that the correlation was most negative, indicating that methylation regulated the mRNA expression of these genes (except for EMX2, LEMD3, ZFP2, ZSCAN1). The results illustrated that the DNA methylation played an significant role in the expression of these genes.

The clinical characteristics and prognosis model of the patient were used as different influencing factors, and the prognostic information of the patient was analyzed by univariate and multivariate cox analyses , and the corresponding ROC curve is drawn. The results of the univariate cox analysis found that the predictive effect of the prognostic model and patient stage was higher than other clinical characteristics(Figure 10A). However the results of multivariate cox analyses showed that only the prognostic model can independently evaluate the prognosis of the patient(Figure 10B).

## 4. Discussion

The incidence of LUSC is high, and its five-year survival rate is less than 15 % [10]. In the past decade, the targeted therapy for LUSC patients has made great progress [11-13]. However, the resistance of targeted drugs and the side effects of treatment have limited the application in therapy. Therefore, in order to increase the survival time of patients and reduce the side effects of drugs, it is urgent to integrate the clinical and related detection information of LUSC patients to identify new early diagnosis biomarkers, find new therapeutic targets, and predict the prognosis of patients. The rapid development of high-throughput sequencing technology has provided valuable data for studying the mechanism of cancer.

Cancer is associated with genetics and epigenetics [14]. In all DNA-based biological processes such as transcription, modification, and replication, epigenetic modification conveys information that can play a crucial regulatory role [15]. Epigenetic changes affect the entire process of tumorigenesis and development by affecting genomic stability and gene expression [16]. Epigenetic changes occur in the early stages of tumor development and can be adjusted by external factors, such as drugs, diet, etc., so the individual's epigenetic analysis may provide valuable information for reducing their risk of cancer [17-19]. DNA methylation, microRNA (miRNA), nucleosome remodeling and histone modification are the main mechanisms of epigenetics [20]. These four mechanisms have been proven to be associated with many diseases including tumors [21].

As an important part of epigenetics, DNA methylation has long become a research hotspot. It seems clear that the silencing expression of tumor suppressor genes caused by methylation may be the origin of important events in tumorigenesis[22]. There is increasing evidence that DNA methylation is associated with lung cancer [23, 24]. Studies have shown that the incidence of H-cadherin methylation in patients with non-small cell lung cancer is significantly related to tumor stage [25]. The methylation levels of VAX1, CH25H, ADCYAP1 and IRX1 genes are related to the prognosis of LUSC patients [10]. Modeling the methylation genes and clinical information of patients through bioinformatics can predict the treatment and prognosis of patients to a certain extent. The model uses 26 related methylation sites, corresponding to 24 related genes. GNAS, FZD2, FZD10 are the core three genes that may be related to the prognosis of

LUSC patients. GNAS mutations have been found in pancreas, colon and lung tumors, and in up to two-thirds of intraductal papillary mucinous tumors (IPMNs) [26-30]. According to the results of in vitro and in vivo experiments, Fzd2 is an oncogene, and overexpression of Fzd2 and signaling through the noncanonical Wnt pathway can promote the development of advanced metastatic cancer [31]. FZD10, a receptor for the Wnt pathway, is associated with the activation of Wnt signaling in colorectal cancer, gastric cancer, and synovial sarcoma, and is expressed at high levels in these cancers[32-34].

In this study, we aimed to build a model that can predict the prognosis of LUSC patients by integrating and analyzing the clinical information of LUSC patients in the TCGA database with the information of the relevant methylation sequencing of the UCSC database. The methylation sites screened out in this study may be used as special diagnostic indicators and potential therapeutic targets for lung squamous cell carcinoma. Further testing the prognosis prediction model constructed in this study, the internal verification results are favourable, but the external verification results are general. By reducing the data of externally verified patients, it is found that the AUC value fluctuates greatly, so it is speculated that the results of external verification may be related to the number of patients and need further verification. Further analysis of the ROC curve of its multi-year survival rate shows that as the survival time increases, the prediction results of the model become more and more accurate. The constructed prediction model integrates methylation sites of independent prognosis, which can be used to evaluate the prognosis of the patient and may assist the clinical treatment of the patient. This model classifies the molecular subtypes of disease in LUSC patients, and provides more individualized treatment recommendations and prognostic evaluation for different clinical subtypes. However, this prediction model also has some problems. First, the model is based on the TCGA database, and the number of LUSC patients is only 504, so the model is still not accurate enough. Secondly, in the clinical treatment of patients, there are many other influencing factors, which will also have a certain impact on the predictive performance of this model. Third, the prediction model is still in its infancy, and there is still a lot of room for improvement. It needs to be further clinically verified and combined with clinical conditions for further improvement.

## 5. Conclusions

In this study, we divided patients into seven molecular subtypes based on their methylation expression levels. Based on the methylation sites of the subcohort with the best prognosis, a model that can be used to evaluate the prognosis of LUSC patients was constructed. After external and internal verification, it is found that with the extension of survival time, its prediction effect shows an upward trend. Our results indicate that DNA methylation plays an important role in the occurrence and development of LUSC and may be proposed as a diagnostic biomarker.

## Abbreviations

LUSC: Lung squamous cell carcinoma; TSG: tumor suppressor genes; AUC: area under curve; ROC curve: receiver operating characteristic curve; T category(T stage):primary tumor; N category(N stage): regional lymph nodes; M category(M stage): distant metastasis. CDF: Cumulative Distribution Function; TCGA: the

Cancer Genome Atlas; UCSC: the University of California Santa Cruz. NSCLC: Non-small cell lung cancer. GO: Gene Ontology; KEGG: Kyoto Encyclopedia of Genes and Genomes.

## Declarations

### Ethics approval and consent to participate

This work did not require ethical approval. All public data sets used were generated by others with ethical approval.

### Consent for publication

Not applicable.

### Availability of data and material

All data generated or analysed during this study are included in this published article.

### Competing interests

The authors declare that they have no conflicts of interest.

### Funding

This work was supported by Project of Administration of Traditional Chinese Medicine of Guangdong Province of China ( Project No. 20201109 ). The funding bodies were not involved in the design of this study or in the collection of data, analysis, and interpretation of hereof.

### Authors' contributions

RSZ, YSH, ZJY and FH conducted experiments, KCN, XSL and ZHZ collected the data and wrote the manuscript. YSH and ZJY conducted experiments. RSZ and FH collected data, contributed to the discussion and reviewed the manuscript. XSL, KCN, ZHZ contributed the same, so they are the first authors. YT are the guarantors of this work and, as such, has full access to all the data in the study and takes responsibility for the integrity of the data and the accuracy of the data analysis. All authors have read and approved the manuscript.

### Acknowledgement

Not Applicable.

## References

1. Bray F, Ferlay J, Soerjomataram I, Siegel RL, Torre LA, Jemal A: **Global cancer statistics 2018: GLOBOCAN estimates of incidence and mortality worldwide for 36 cancers in 185 countries.** *CA: a*

- cancer journal for clinicians* 2018, **68**(6):394-424.
2. Hong QY, Wu GM, Qian GS, Hu CP, Zhou JY, Chen LA, Li WM, Li SY, Wang K, Wang Q *et al*. **Prevention and management of lung cancer in China.** *Cancer* 2015, **121** Suppl 17:3080-3088.
  3. Wood K, Hensing T, Malik R, Salgia R: **Prognostic and Predictive Value in KRAS in Non-Small-Cell Lung Cancer: A Review.** *JAMA Oncol* 2016, **2**(6):805-812.
  4. Wang X, Shang W, Chang Y, Li X: **Methylation Signature Genes Identification of the Lung Squamous Cell Carcinoma Occurrence and Recognition Research.** *J Comput Biol* 2018, **25**(10):1161-1169.
  5. Duruisseaux M, Esteller M: **Lung cancer epigenetics: From knowledge to applications.** *Semin Cancer Biol* 2018, **51**:116-128.
  6. Jones MJ, Goodman SJ, Kobor MS: **DNA methylation and healthy human aging.** *Aging Cell* 2015, **14**(6):924-932.
  7. Belinsky SA: **Silencing of genes by promoter hypermethylation: key event in rodent and human lung cancer.** *Carcinogenesis* 2005, **26**(9):1481-1487.
  8. Esteller M: **Epigenetics in cancer.** *N Engl J Med* 2008, **358**(11):1148-1159.
  9. Heyn H, Esteller M: **DNA methylation profiling in the clinic: applications and challenges.** *Nat Rev Genet* 2012, **13**(10):679-692.
  10. Gao C, Zhuang J, Zhou C, Ma K, Zhao M, Liu C, Liu L, Li H, Feng F, Sun C: **Prognostic value of aberrantly expressed methylation gene profiles in lung squamous cell carcinoma: A study based on The Cancer Genome Atlas.** *J Cell Physiol* 2019, **234**(5):6519-6528.
  11. Drilon A, Rekhtman N, Ladanyi M, Paik P: **Squamous-cell carcinomas of the lung: emerging biology, controversies, and the promise of targeted therapy.** *Lancet Oncol* 2012, **13**(10):e418-426.
  12. Lee CK, Brown C, Gralla RJ, Hirsh V, Thongprasert S, Tsai CM, Tan EH, Ho JC, Chu da T, Zaatar A *et al*: **Impact of EGFR inhibitor in non-small cell lung cancer on progression-free and overall survival: a meta-analysis.** *J Natl Cancer Inst* 2013, **105**(9):595-605.
  13. Sun Y, Han Y, Wang X, Wang W, Wang X, Wen M, Xia J, Xing H, Li X, Zhang Z: **Correlation of EGFR Del 19 with Fn14/JAK/STAT signaling molecules in non-small cell lung cancer.** *Oncol Rep* 2016, **36**(2):1030-1040.
  14. Baylin SB, Jones PA: **A decade of exploring the cancer epigenome - biological and translational implications.** *Nat Rev Cancer* 2011, **11**(10):726-734.
  15. Dawson MA, Kouzarides T: **Cancer epigenetics: from mechanism to therapy.** *Cell* 2012, **150**(1):12-27.
  16. Brassat E, Chambeyron SJGB: **Epigenetics and transgenerational inheritance.** 2013, **14**(5).
  17. Hou L, Zhang X, Wang D, Baccarelli A: **Environmental chemical exposures and human epigenetics.** *Int J Epidemiol* 2012, **41**(1):79-105.
  18. Costa FJCM, Research: **Epigenomics in cancer management.** 2010.
  19. Verma MJCOiCN, Care M: **Cancer control and prevention: Nutrition and epigenetics.** 2013.
  20. Jones P: **Out of Africa and into epigenetics: discovering reprogramming drugs.** *Nat Cell Biol* 2011, **13**(1):2.

21. Feinberg APJVAIJOP: **Genome-scale approaches to the epigenetics of common human disease.** 2010, **456**(1):p.13-21.
22. Gao A, Guo M: **Epigenetic based synthetic lethal strategies in human cancers.** *Biomarker research* 2020, **8**:44.
23. Chakravarthi BV, Nepal S, Varambally S: **Genomic and Epigenomic Alterations in Cancer.** *Am J Pathol* 2016, **186**(7):1724-1735.
24. Huang T, Chen X, Hong Q, Deng Z, Ma H, Xin Y, Fang Y, Ye H, Wang R, Zhang C *et al.*: **Meta-analyses of gene methylation and smoking behavior in non-small cell lung cancer patients.** *Sci Rep* 2015, **5**:8897.
25. Kim JS, Han J, Shim YM, Park J, Kim DH: **Aberrant methylation of H-cadherin (CDH13) promoter is associated with tumor progression in primary nonsmall cell lung carcinoma.** *Cancer* 2005, **104**(9):1825-1833.
26. Wu J, Matthaehi H, Maitra A, Dal Molin M, Wood LD, Eshleman JR, Goggins M, Canto MI, Schulick RD, Edil BH *et al.*: **Recurrent GNAS mutations define an unexpected pathway for pancreatic cyst development.** *Sci Transl Med* 2011, **3**(92):92ra66.
27. Fecteau RE, Lutterbaugh J, Markowitz SD, Willis J, Guda K: **GNAS mutations identify a set of right-sided, RAS mutant, villous colon cancers.** *PLoS One* 2014, **9**(1):e87966.
28. Springer S, Wang Y, Dal Molin M, Masica DL, Jiao Y, Kinde I, Blackford A, Raman SP, Wolfgang CL, Tomita T *et al.*: **A combination of molecular markers and clinical features improve the classification of pancreatic cysts.** *Gastroenterology* 2015, **149**(6):1501-1510.
29. Kadayifci A, Atar M, Wang JL, Forcione DG, Casey BW, Pitman MB, Brugge WR: **Value of adding GNAS testing to pancreatic cyst fluid KRAS and carcinoembryonic antigen analysis for the diagnosis of intraductal papillary mucinous neoplasms.** *Dig Endosc* 2017, **29**(1):111-117.
30. Ritterhouse LL, Vivero M, Mino-Kenudson M, Sholl LM, Iafrate AJ, Nardi V, Dong F: **GNAS mutations in primary mucinous and non-mucinous lung adenocarcinomas.** *Mod Pathol* 2017, **30**(12):1720-1727.
31. Singh I, Mehta A, Contreras A, Boettger T, Carraro G, Wheeler M, Cabrera-Fuentes HA, Bellusci S, Seeger W, Braun TJBB: **Hmga2 is required for canonical WNT signaling during lung development.** 2014, **12**(1):21.
32. Koike J, Takagi A, Miwa T, Hirai M, Terada M, Katoh MJB, Communications BR: **Molecular Cloning of Frizzled-10, a Novel Member of the Frizzled Gene Family.** 1999, **262**(1):0-43.
33. Fukukawa C, Nagayama S, Tsunoda T, Toguchida J, Nakamura Y, Katagiri TJO: **Activation of the non-canonical Dvl–Rac1–JNK pathway by Frizzled homologue 10 in human synovial sarcoma.** 2009, **28**(8):1110-1120.
34. Nagayama S, Yamada E, Kohno Y, Aoyama T, Fukukawa C, Kubo H, Watanabe G, Katagiri T, Nakamura Y, Sakai YJCS: **Inverse correlation of the up-regulation of FZD10 expression and the activation of  $\beta$ -catenin in synchronous colorectal tumors.** 2009, **100**(3).

## Figures

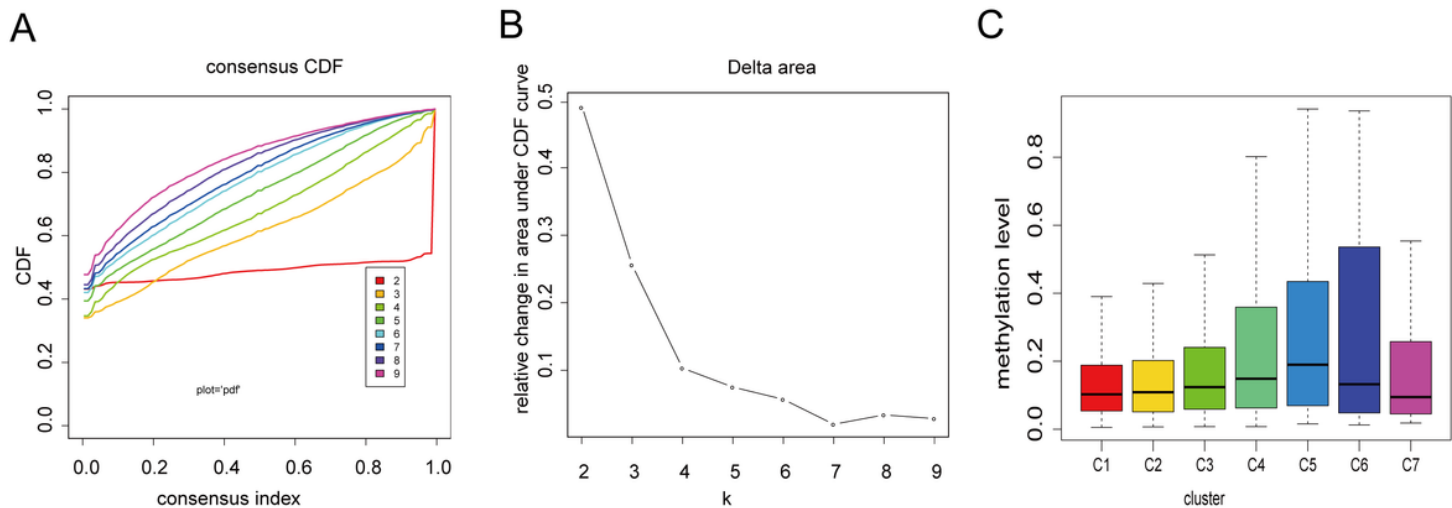


**Figure 1**

Standard for choosing amount of subtypes. (A) Consensus among subtypes for each cluster number  $k$ . (B) The Delta area curve used for consensus clustering represents under the CDF curve the relative change in the area for each cluster number  $k$  compared to  $k-1$ . The category number  $k$  is indicated by the horizontal axis coordinate, and the relative change of the area under the CDF curve is indicated by the vertical axis coordinate. (C) Box plot of CpG methylation levels of the 7 Clusters.

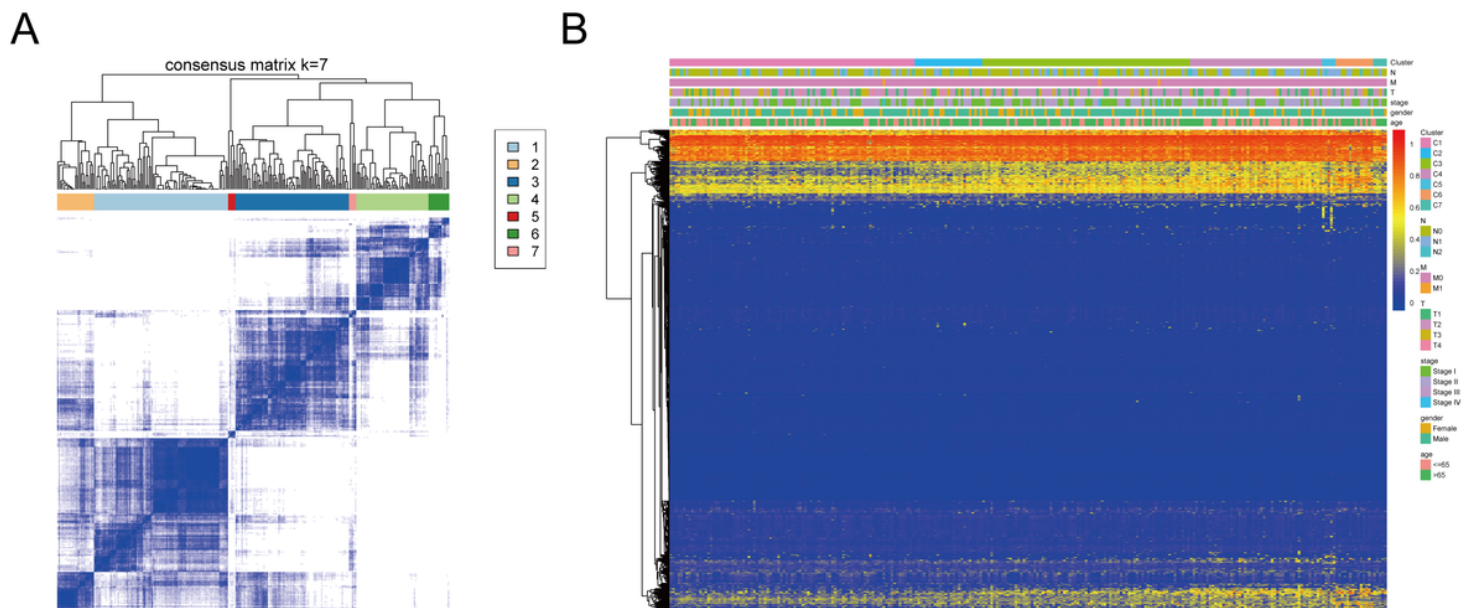


**Figure 2**

Consensus matrix and corresponding heat map of DNA methylation subtypes. (A) Color-coded heatmap which corresponds to the consensus matrix( $k=7$ ) gained by processing consensus clustering. Use a color gradient to indicate the consensus value from 0 (white) to 1 (dark blue). (B) A heatmap which corresponds to the Figure 2A with the annotation of the DNA methylation subtypes, stage, age and TNM category.

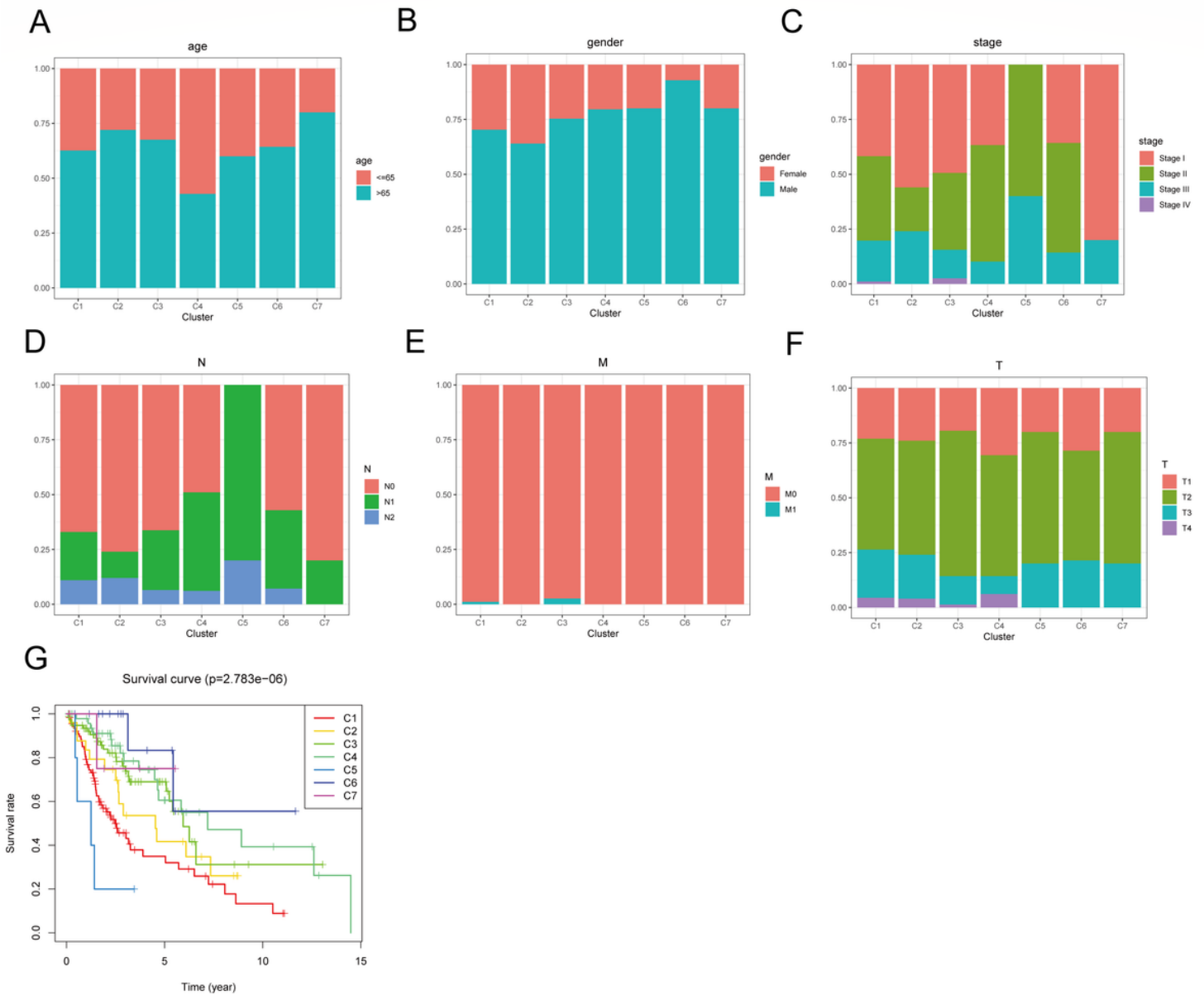


**Figure 3**

Comparison of age, gender, stage, TNM stage and prognosis among the DNA methylation subtypes. Figures A, B, C, D, E, and F represent age, gender, stage score, topography score, lymphocyte infiltration and metastasis distributions for every DNA methylation cluster in the training set. The DNA methylation subtypes are represented by the coordinates of the horizontal axis. (G) Survival curves for every DNA methylation cluster in the training group. The survival time (years) is represented by the horizontal axis, and the survival probability is represented by the vertical axis. Use the log-rank test to evaluate the statistical significance of differences among clusters.

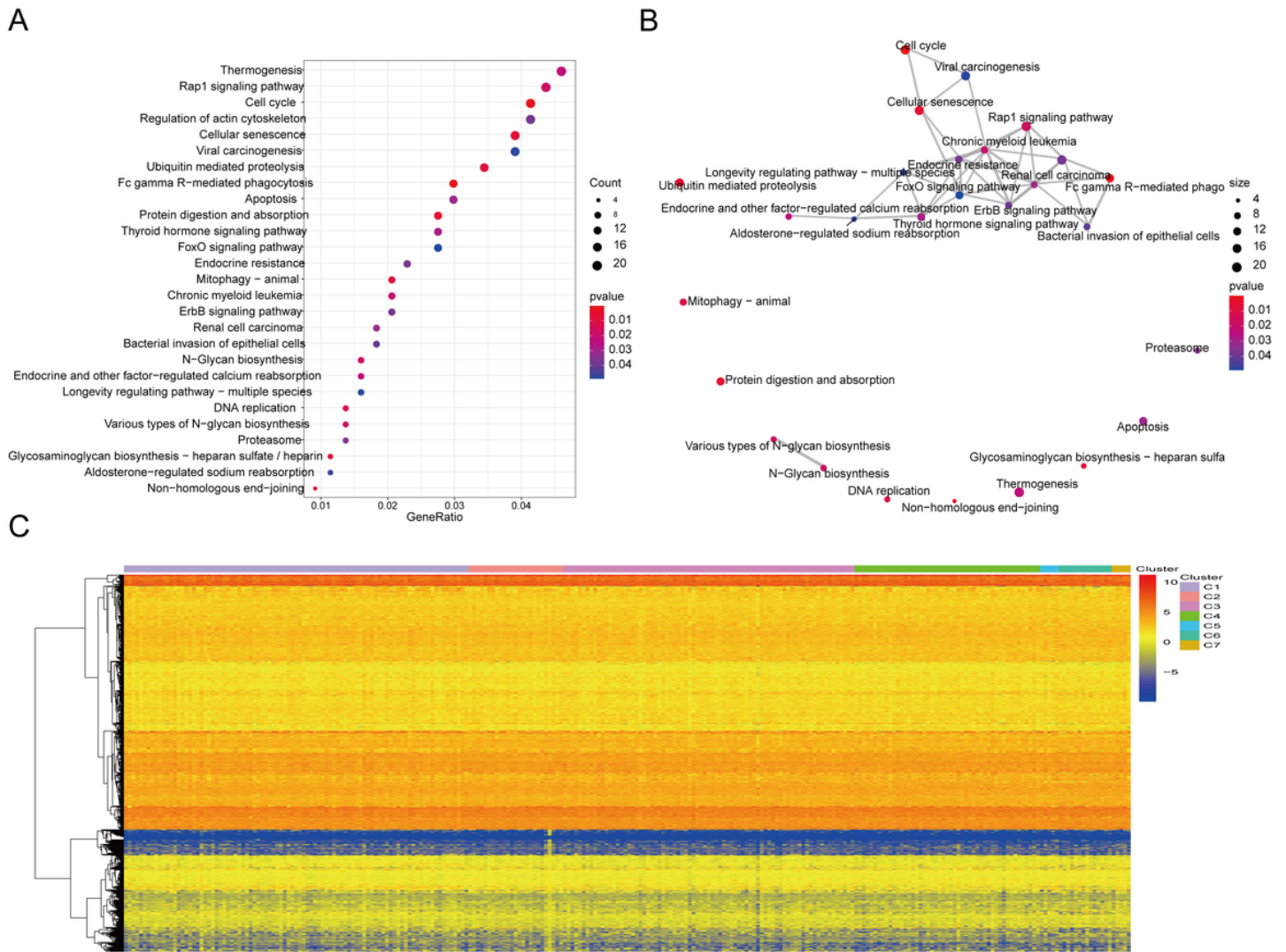


**Figure 4**

Gene annotations of 965 methylated sites. (A) KEGG pathway enrichment analysis of annotated 1037 genes for the 965 CpG sites. (B) Crosstalk analysis of the results from KEGG pathways enrichment analysis using "Enrichment" R package. (C) Cluster analysis heat map for annotated genes associated with the 966 CpG sites

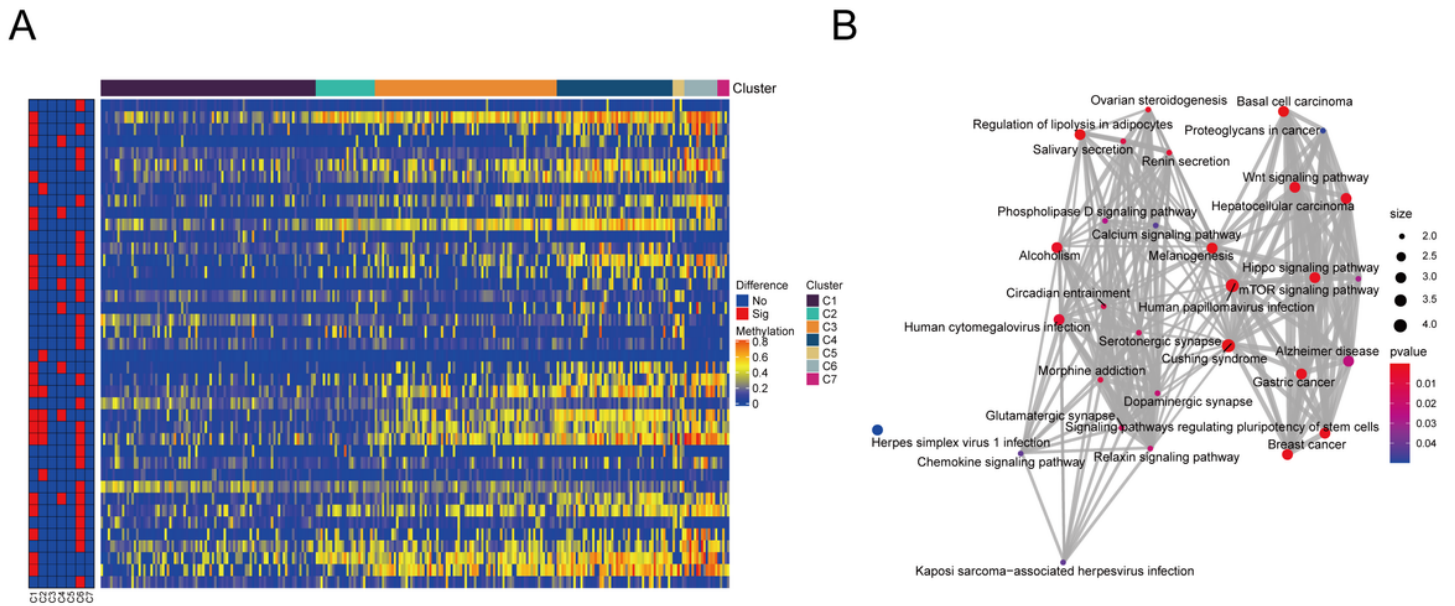


**Figure 5**

Specific hypo/hyper-methylation CpG sites for every DNA methylation cluster. (A) Specific CpG sites are displayed for every DNA methylation prognosis subtype. Hypo- and hypermethylation CpG sites are represented by red and blue bars. (B) Crosstalk analysis of the results from KEGG pathways enrichment analysis using "Enrichment" R package.

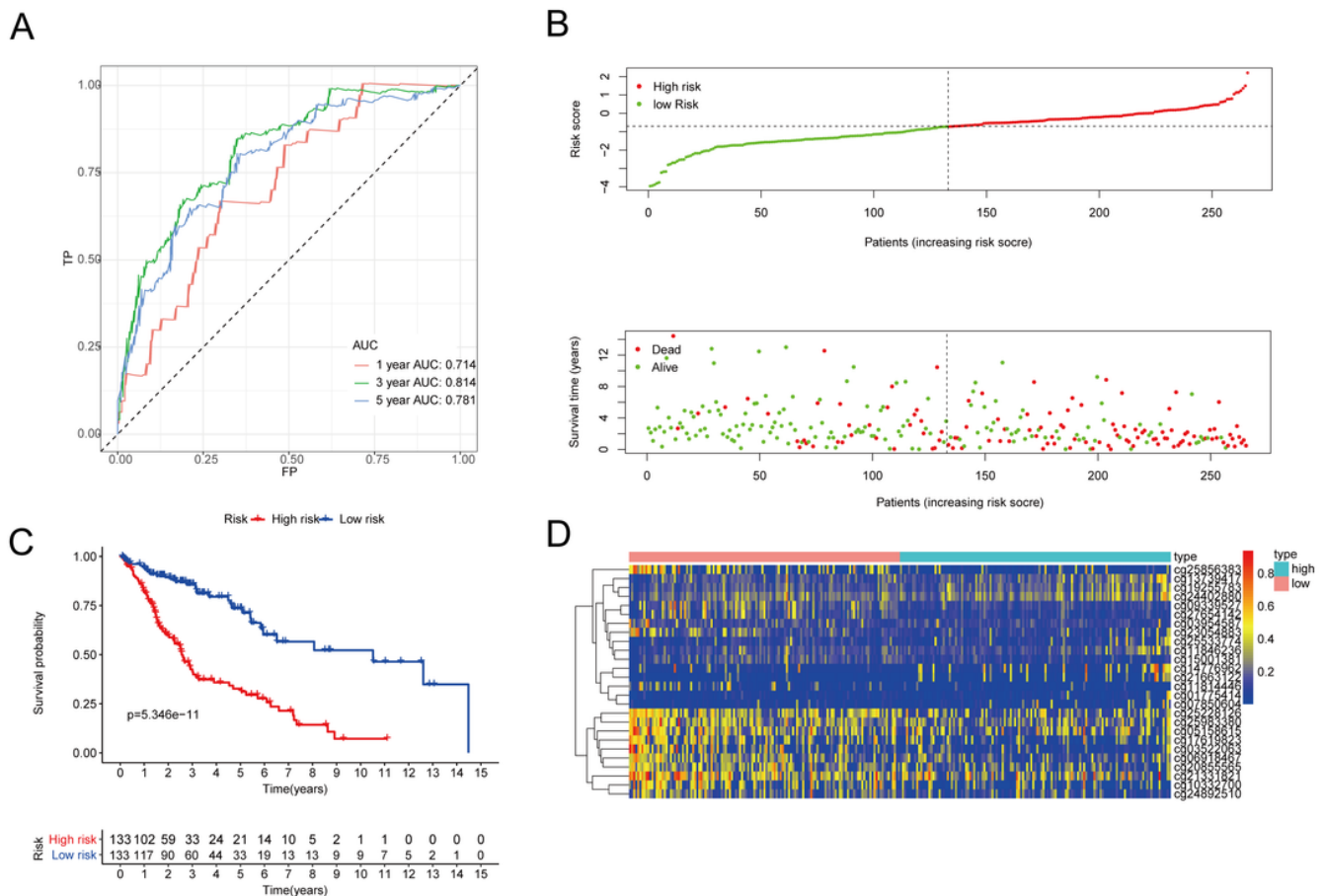


**Figure 6**

Construction of the model for forecasting prognosis of LUSC patients in the external train group. (A) The ROC curve of the prognostic indicators of 1 year, 3 years and 5 years. (B) The horizontal axis represents patient samples, and the vertical axis represents the risk score (upper) and the overall survival(lower). (C) Prognostic difference analysis between high-risk group and low-risk group. (D) The Heat map showing the expression levels of 26 methylation sites which were used to build the prognostic model in the high-risk and low-risk groups in external train group.

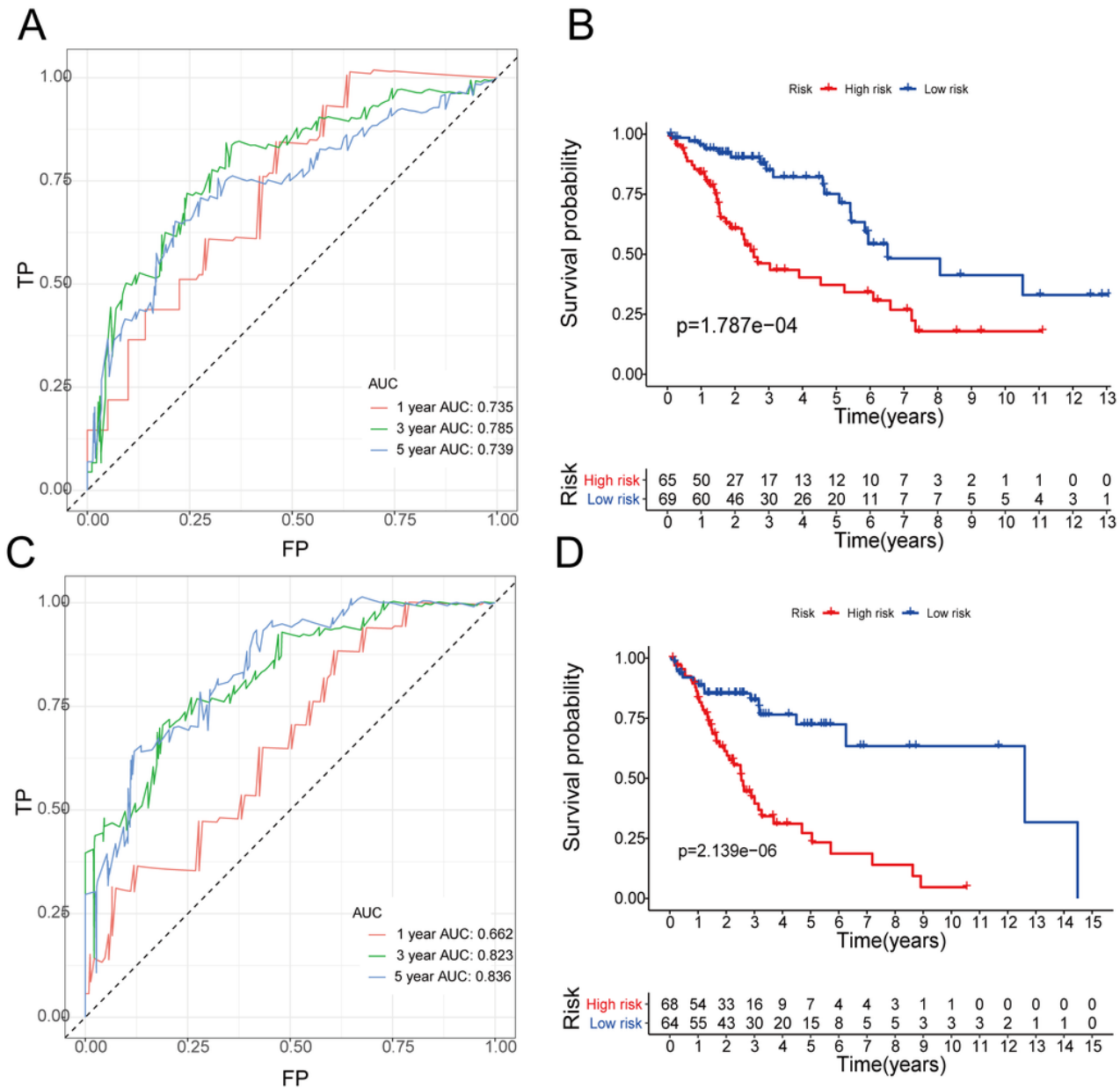


**Figure 7**

Construction and internal verification of the model for forecasting prognosis of LUSC patients. (A) ROC curves of prognostic predictors in the internal training group. (B) Prognostic difference analysis between high-risk group and low-risk group in the internal training group. (C) ROC curves of prognostic predictors

in the internal testing group. (D) Prognostic difference analysis between high-risk group and low-risk group in the internal testing group.

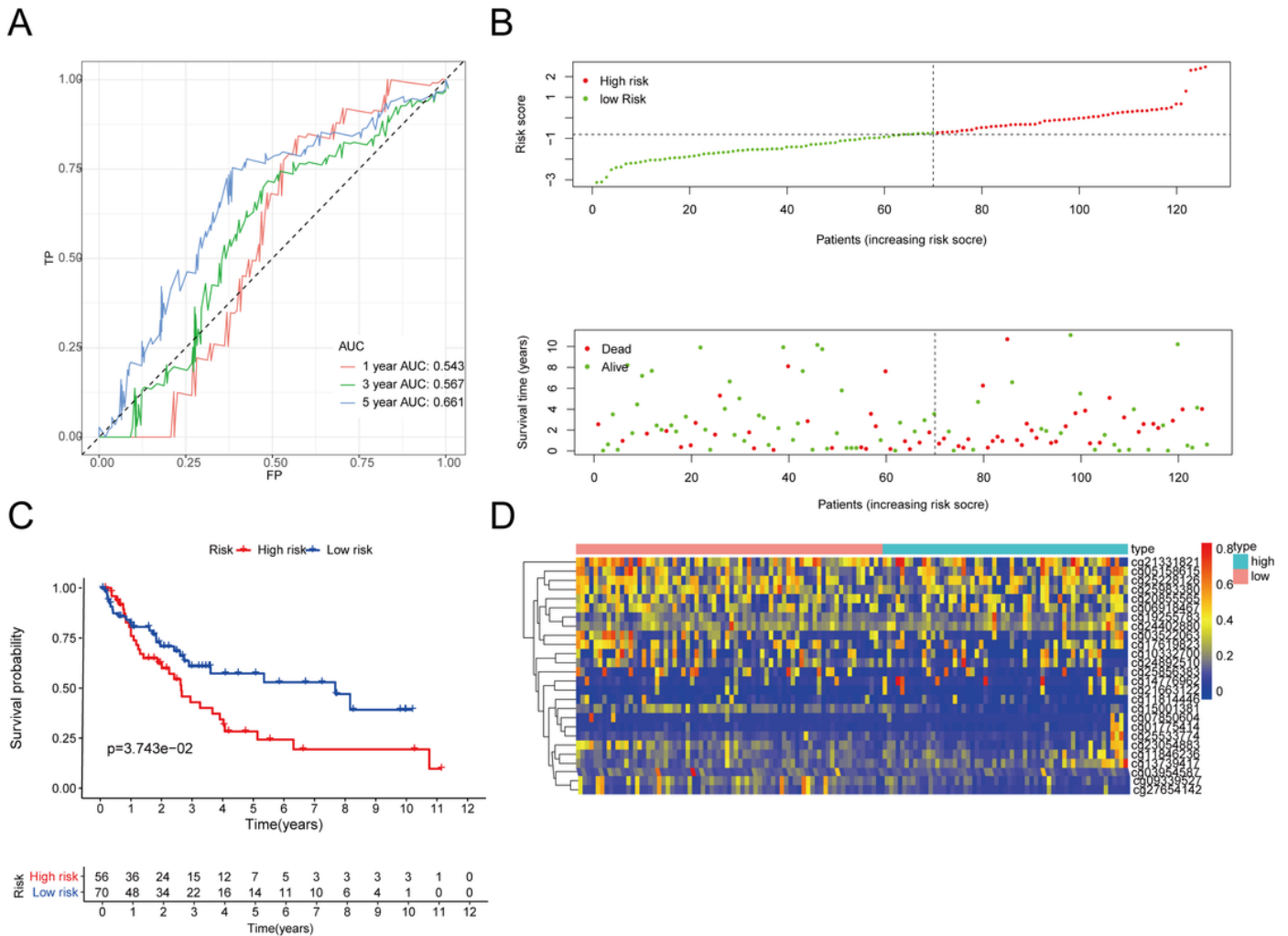


**Figure 8**

Construction of the model for forecasting prognosis of LUSC patients in the external test group. (A) The ROC curve of the prognostic indicators of 1 year, 3 years and 5 years. (B) The horizontal axis represents patient samples, and the vertical axis represents the risk score (upper) and the overall survival (lower). (C) Prognostic difference analysis between high-risk group and low-risk group. (D) The Heat map showing the expression levels of 26 methylation sites which were used to build the prognostic model in the high-risk and low-risk groups in external test group.

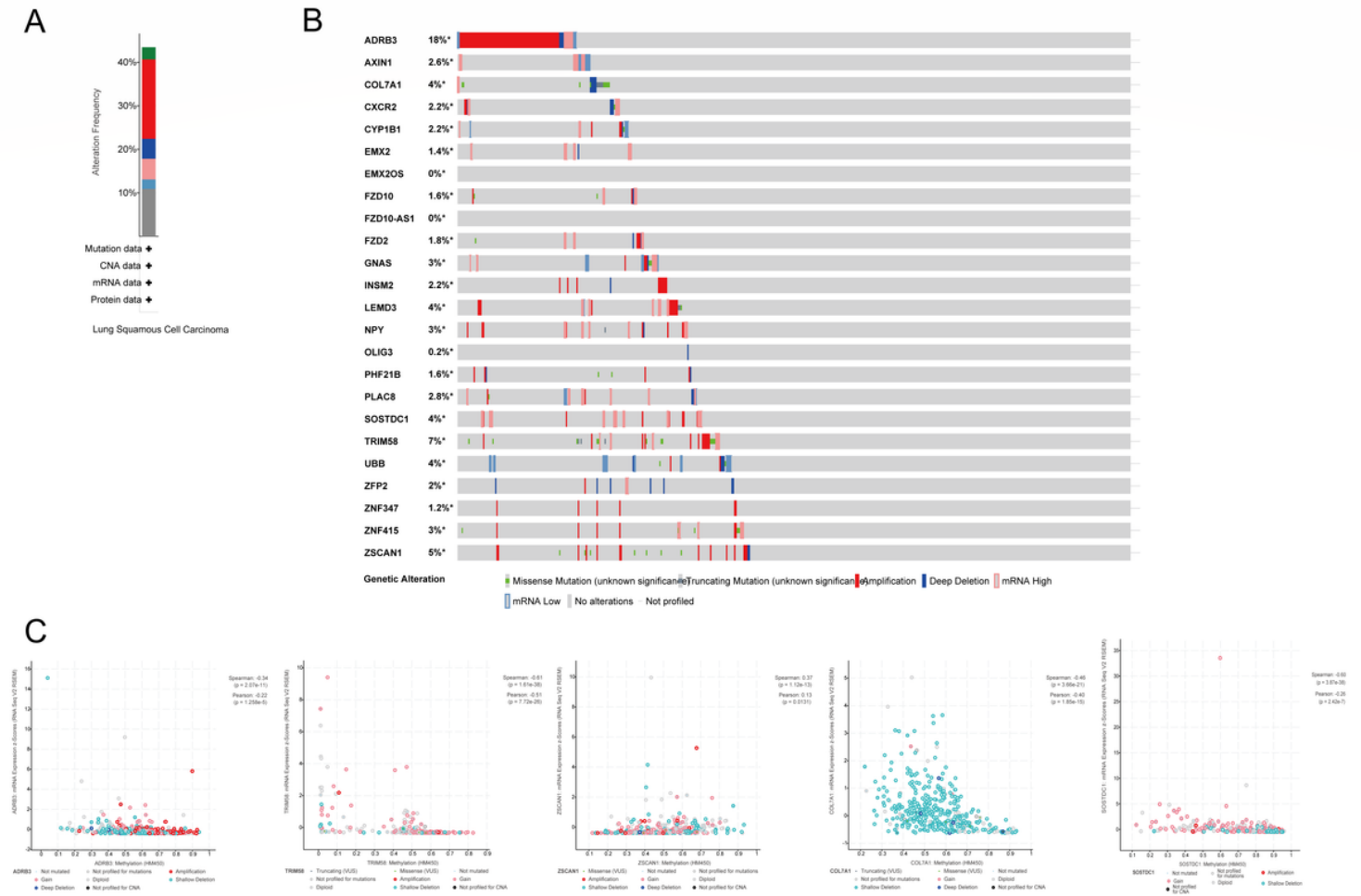


**Figure 9**

The genetic alterations associated with 24 genes and the correlation between mRNA and DNA methylation. (A) The spliced bar graph summarizes and displays the genetic variation of 24 genes in 43% of the sequenced cases/patients (511 in total). (B) The specific genetic variation of 24 genes in the TCGA lung cancer dataset. (C) The correlation between DNA methylation and mRNA of top 5 genes in the TCGA lung cancer dataset.

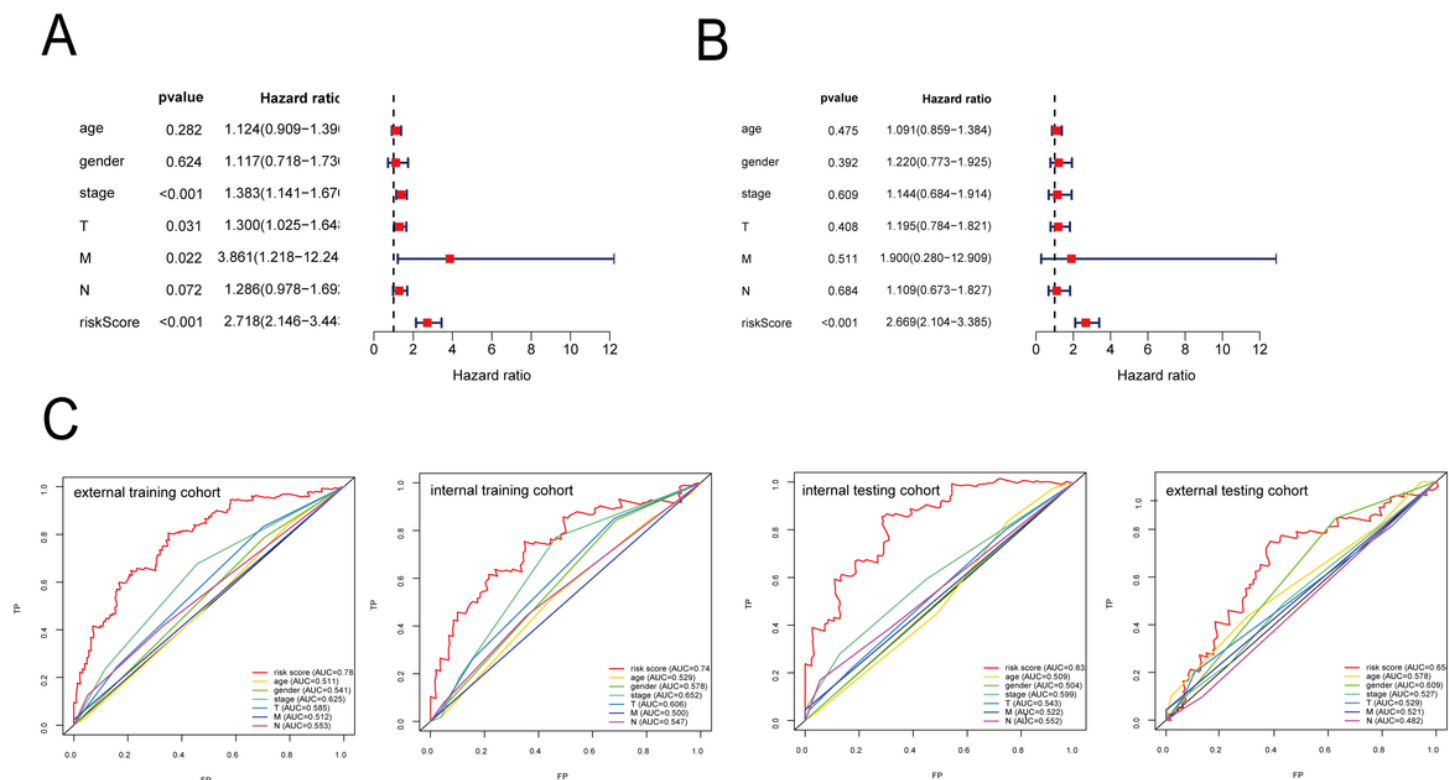


**Figure 10**

Independent predictive power of the prognosis model for lung squamous cell carcinoma. (A) Univariate Cox analysis. (B) Multivariate Cox analysis. (C) AUC in ROC analysis for prognosis model and clinical characteristics in the signature at the 5-year survival time in four cohorts.

## Supplementary Files

This is a list of supplementary files associated with this preprint. Click to download.

- [AppendixS1.xlsx](#)
- [AppendixS2.xlsx](#)
- [AppendixS3.xlsx](#)
- [AppendixS4.xlsx](#)
- [AppendixS5.xlsx](#)
- [AppendixS6.xlsx](#)
- [AppendixS7.xlsx](#)
- [AppendixS8.xlsx](#)
- [AppendixS9.xlsx](#)
- [AppendixS10.xlsx](#)
- [AppendixS11.xlsx](#)